Contents lists available at ScienceDirect

Arabian Journal of Chemistry

journal homepage: www.ksu.edu.sa

Original article

Highly dispersed palladium nanoparticles decorated on nitrogen doped graphene for enhanced photoelectrochemical water splitting

Mohammed Rafi Shaik [a], Maha Al-Othman [a], Mufsir Kuniyil [a], Abdulrahman Al-Warthan [a], Mohammad Rafe Hatshan [a], Mohamed E. Assal [a], Muhammad Nawaz Tahir [b,c], Mujeeb Khan [a,*]

[a] Department of Chemistry, College of Science, King Saud University, P.O. Box 2455, Riyadh 11451, Saudi Arabia
[b] Chemistry Department, King Fahd University of Petroleum & Minerals, Dhahran 31261, Kingdom of Saudi Arabia
[c] Interdisciplinary Research Center for Hydrogen Technologies and Carbon Management (IRC-HTCM), King Fahd University of Petroleum & Minerals KFUPM, Dahran 31261, Saudi Arabia.

ARTICLE INFO

Keywords:
Metallic NPs
Nitrogen doped graphene
Nanocomposite
Electrocatalysts
Hydrogen evaluation

ABSTRACT

Among various clear energy generation processes, electrocatalytic water splitting or hydrogen evolution reaction (HER) has been considered as an efficient method for the sustainable production of hydrogen (H_2) fuel. But, significant efforts are still required to develop cheap, effective and stable electrocatalysts for water splitting to achieve the economical production of H_2. In the quest of finding cheap electrocatalysts, herein, we demonstrate the preparation of palladium (Pd) nanoparticles decorated nitrogen (N) doped highly reduced graphene oxide (NDG-Pd) based electrocatalysts. The nitrogen (N) doped highly reduced graphene oxide (NDG) was produced by using graphene oxide as precursor, which was reduced and doped with nitrogen, simultaneously in one-step hydrothermal method. Subsequently, Pd nanoparticles were decorated on the surface of NDG using a facile ultrasonic method to produce NDG-Pd. In order to restrict the amount of precious metal to reduce the cost of catalysts, very small percentage of Pd, such as, 1 and 3 % was utilized during the preparation of electrocatalysts. The as-prepared electrocatalysts were successfully characterized by using different methods such as, XRD, XPS, EDX, BET, SEM and TEM. Results confirmed the formation of slightly agglomerated, smaller size of Pd NPs on the surface of NDG with an average particle size of ~ 6 nm. The as prepared nanocomposites NDG, NDG-Pd1% and NDG-Pd3% were used to prepare electrodes and their electrocatalytic activity was evaluated towards the production of H_2 through water splitting. The results of electrochemical performance of as-prepared electrodes within the voltage range have revealed that among different samples prepared, the NDG did not show any current, whereas NDG-Pd3% showed a good potential for HER with current density ≈24 mA/cm^2 at very low potential i.e. −0.2 V vs RHE.

1. Introduction

Currently, the rapid depletion of fossil fuels has significantly increased the demand for the development of alternative energy technologies (Qazi et al., 2019; Zhang et al., 2024). This has led to lavish utilization of various sustainable energy resources, such as, wind, solar and water resources for the generation of easily accessible and affordable energy (Ashraf et al., 2021; Hassan et al., 2024; Hussain et al., 2017). Among various renewable energy technologies, the production of hydrogen and oxygen via photocatalytic water splitting and natural renewable sources such as biomass, plastic etc. has gained significant traction in the scientific community (Ashraf et al., 2023c; Fajrina and Tahir, 2019). This method has great potential in the production of renewable energy without depending on fossil fuels and with zero emission (Dharmarajan et al., 2024; Li and Tsang, 2020). Particularly, hydrogen (H_2) generation from water using light source has been established as an effective process to produce clean energy which can play crucial role in solving the global energy crisis and environmental issues, simultaneously (Ashraf et al., 2023a; Ashraf et al., 2023b; Lin et al., 2020; Rauf et al., 2024). H_2 energy is considered as clean and economical energy and thus has gained significant prominence due to its abundance, easy storage, enormous environmental and climate benefits (Sikiru et al., 2024; Yue et al., 2021). In this regard, electrocatalytic water splitting is among the most promising approaches for converting

* Corresponding author.
E-mail address: kmujeeb@ksu.edu.sa (M. Khan).

https://doi.org/10.1016/j.arabjc.2024.105718
Received 2 January 2024; Accepted 6 March 2024
Available online 7 March 2024

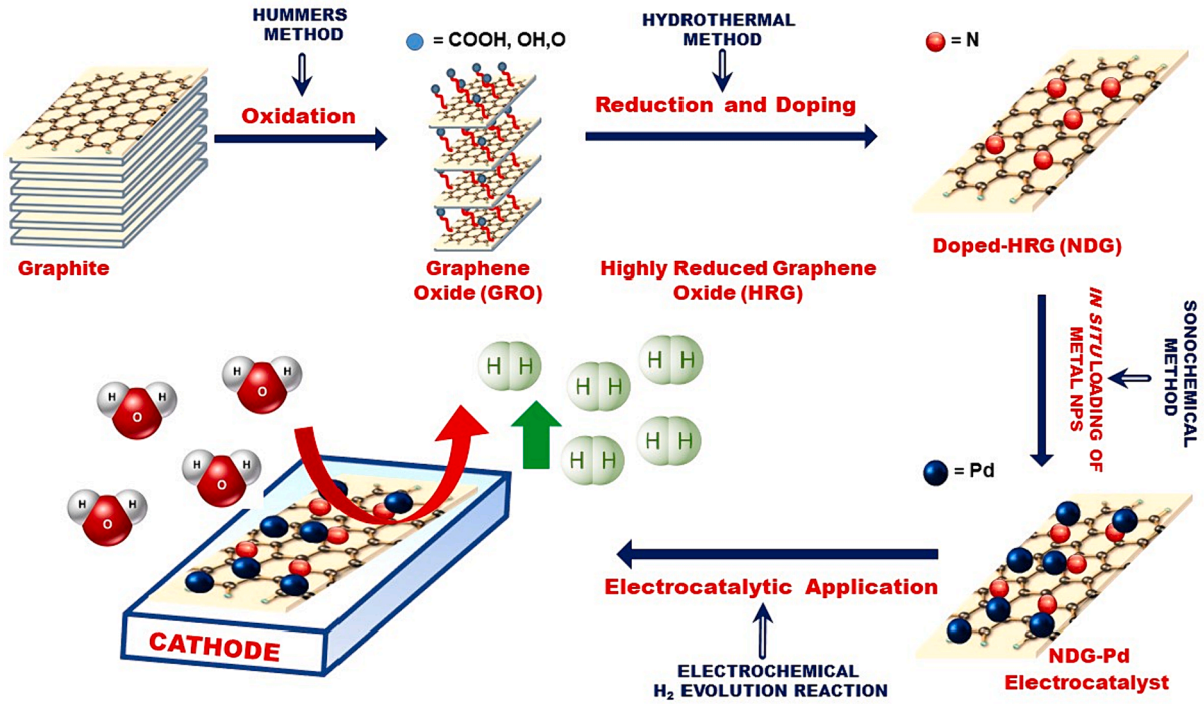

Scheme 1. Schematic representation of the preparation of the nitrogen doped graphene and Pd based nanocomposites and their electrocatalytic application for the production of H_2 via water splitting.

solar energy to clean H_2 energy (Sun et al., 2024; Wang et al., 2019).

Although, electrocatalytic H_2 production via water splitting delivers high conversion efficiency in comparison to the photocatalytic approaches, still, there are several limitations which inhibit the large-scale implementation of this process (Gao et al., 2024; Li et al., 2021). Nevertheless, considerable research has been performed over several decades to address the lingering issues of electrocatalytic H_2 evolution, such as, increasing the rate of H_2 production, improving the catalytic activities of electrocatalysts (Hanan et al., 2024; Khan et al., 2023; Margarit et al., 2021). Usually, platinum-based materials have long been considered as effective electrocatalysts in water splitting, due to their low overpotential, enhanced electrocatalytic stability (Jeong et al., 2022). However, the low abundance of platinum and relatively high cost has mainly inhibited the large-scale applications of platinum-based materials for H_2 generation (Han et al., 2024; Zhong et al., 2021). Therefore, the development of cheap, high performance, alternative electrocatalysts is the need of the hour for the sustainable production of H_2 via water splitting (Abbas and Bang, 2015; Chen et al., 2024). Although as replacement to precious metals, metal-free and non-metallic single atom based electrocatalyst are gradually gaining traction (Zhang et al., 2023). But, these substances generally require expensive and tedious synthesis processes which is unfavorable for practical application (Zhao et al., 2019). On the other hand, the electrocatalytic efficiency of precious metals including Pt, Pd, Au etc., is still unmatched (Huang et al., 2024; Lyu et al., 2019; Zhang and Dai, 2024). Moreover, the size of metallic NPs also play critical role in the electrochemical reactions, since, smaller size NPs exhibit relatively large number of surface atoms, which may enhance the molecular absorption during reactions (Hayden, 2013). Typically, metallic NPs including Pt and Pd in the size range of 3 to 5 nm have been reported to be the most active electrocatalysts (Tang and Cheng, 2015).

To address the issues with precious metals, researchers have either reduced the amount of noble metal (Pt.) in the electrocatalysts, or it is completely replaced with less expensive and/or nonprecious metals based electrocatalysts (Ibn Shamsah, 2021; Jiang et al., 2024). For instance, as a replacement to platinum, relatively cheap and readily available metals-based materials (with less contents of active metal) like palladium, gold, copper etc., have been applied (Smiljanić and Grgur, 2024; Yi et al., 2018). Besides, the content of active metal can be reduced by the utilization of suitable support, which not only help to compensate the amount of precious metal, but also offer strength to the catalyst (Zhang et al., 2019). Moreover, as the catalysis is a surface phenomenon, only the metallic components present on the surface of the catalysts play active role during the reaction (Vogt and Weckhuysen, 2022). Among various precious metals, palladium (Pd) is regarded as relatively cheap alternative to Pt, which potentially exhibit, efficient electrocatalytic properties and strong stability under electrochemical conditions (Gupta et al., 2024; Wang et al., 2021). Pd based materials have been excessively used as electrocatalysts for various electrocatalytic processes including formic acid oxidation, fuel cells and so on (Shen et al., 2020). However, despite of its high affinity towards H_2, when compare to the other 3d transition elements, Pd based materials have been relatively less explored for electrocatalytic H_2 production (Mahesh et al., 2016).

Regardless of several benefits, Pd also possess various challenges including the aggregation of active nanoparticles in electrocatalysts, loss of stability etc., which negatively impact the surface area and reduce the performance of the materials (Kim et al., 2022). Common approaches to mitigate these effects include alloying the Pd with other metals and application of carbon support materials which prevent the aggregation of particles and enhances the stability of electrocatalysts (Narreddula et al., 2019). So far, a variety of carbon materials have been effectively utilized as efficient supports for Pd based electrocatalysts for H_2 production, including, activated carbon, graphite oxide, highly reduced graphene oxide and heteroatoms doped graphene etc (Al-Rawashdeh et al., 2018). Among these, graphene has been established as wonder support for electrocatalysts in electrochemical energy systems due to its extraordinary properties including excellent electrical conductivity, enhanced durability and high specific surface area (Adil et al., 2022; Liu et al., 2022; Ma et al., 2024).

For instance, Pd NPs which are highly active for methanol and formic acid oxidation than Pt, were successfully deposited with graphene

through redox reaction, the resulting nanocatalyst showed high electrocatalytic ability (Chen et al., 2011). In another study, Ag/graphene was used as a support to deposit hollow PdAg nanorings to obtain a hybrid electrocatalyst. The resulting graphene supported electrocatalysts not only showed high electrocatalytic activity for the ORR but also exhibited remarkably high tolerance towards methanol crossover (Liu et al., 2013). Additionally, heteroatom doped graphene (N, S, B etc.) as support to electrocatalysts has also offered encouraging results in electrochemical processes, these atoms which replace some of the carbon atoms from graphitic lattice introduce defects in the structure (Duan et al., 2015; Liu et al., 2015). These defects not only enhance the chemical stability of the material, but also facilitate rapid electron transfer and increased the surface area of the resulting electrocatalysts (Jiao et al., 2016). Especially, nitrogen doping of graphene matrix significantly enhances the electronic properties of the doped material, due to the possibility of conjugation of π electron of carbon network with the lone pair electron of nitrogen (Dumont et al., 2019) (Saini et al., 2024). The rapid movement of electrons in N-doped graphene generate more active sites on the surface of the catalyst and also enhance the stability of the doped electrocatalysts.

Therefore, in this study, we have prepared N-doped graphene using graphene oxide as precursor, which successfully decorated with different contents of palladium (Pd) nanoparticles. Both the reduction of graphene oxide and doping with nitrogen was performed simultaneously in a facile, one-step hydrothermal approach to obtain N-Doped highly reduced graphene oxide (NDG). Subsequently, different contents of Pd nanoparticles were deposited on the surface of N-Doped HRG via ultrasonication to produce NDG and Pd based nanocomposites (NDG-Pd). The as-prepared NDG-Pd nanocomposites were extensively characterized using XRD, XPS, EDX, SEM, and HR-TEM. The electrochemical activities of the as-prepared Pd based electrocatalysts were tested towards the electrocatalytic production of H_2 via water splitting (cf. Scheme 1). The performance and durability of NDG-Pd electrocatalysts was analyzed by linear sweep voltammetry using electrodes made-up of NDG, NDG-Pd1% and NDG-Pd3%. The performance of the electrodes was evaluated for their potential to electrochemical hydrogen evolution reaction (HER) to produce hydrogen. The electrochemical measurements were performed using a three-electrode system with Pt wire and Ag/AgCl (3 M KCl) electrode were used as counter and reference electrodes respectively.

2. Materials and methods

2.1. Preparation of N-doped highly reduced graphene oxide (NDG)

For this study, graphene oxide was prepared from pristine graphite powder as precursor using a reported modified Hummers method (Khan et al., 2020). In order to prepare, N-doped HRG, freshly prepared graphene oxide (100 mg) was dispersed in 20 ml DI water via sonication (15 min). To this dispersion, 4 ml ammonium hydroxide (NH_4OH) was added and the pH was adjusted to 11, and subsequently, 3 ml of hydrazine hydride was also poured into the mixture while stirring (15 min). The mixture is then transferred to 100 ml Teflon cup, which is fitted into a stainless-steel autoclave. The autoclave was kept in a furnace at a temperature of 150 °C for 24 h. Thereafter, the reaction was stopped and the autoclave was allowed to cool down at room temperature. The product was isolated via centrifugation (8000 rpm, 15 min), which is washed several times with DI water and dried at 65 °C for 12 h to obtain fine black powder.

2.2. Preparation of NDG and palladium nanocomposites (NDG-Pd)

The NDG-Pd composites were prepared by varying the contents of palladium on the surface of NDG i.e., two different samples were prepared by using 1 wt% and 3 wt% of Pd with respect to NDG. Here we only describe the preparation of NDG-Pd with 3 wt% of Pd (NDG-Pd-3 %) in the sample, remaining samples were prepared by using the same procedure by varying the amount of Pd precursor during the synthesis. To prepare NDG-Pd-3 %, 50 mg of NDG was dispersed in 25 ml of ethanol via sonication for 15 min. Separately, 1.5 mg of Na_2PdCl_4 (0.00845 mmol) was dissolved by stirring in 10 ml of ethanol. Subsequently, both the mixtures were mixed together and the resultant mixture was subjected to sonication by using a probe sonicator (Biologics Inc, 3000MP, ultrasonic homogenizer) for 15 min. Thereafter, the product was separated by centrifugation (9000 rpm), washed two times with ethanol and re-dispersed in 10 ml of ethanol for further use. The technical details of the instruments used during the study is provided in the supplementary information.

2.3. Materials characterization

The crystallinity of the as-prepared materials was analyzed via powder X-ray diffraction (XRD) using a D2 Phaser X-ray diffractometer (Bruker, Germany) and Cu Ka radiation (k = 1.5418 A°). Fourier transform infrared (FT-IR) spectra were measured on a Perkin Elmer, 1000 FT-IR spectrometer, (Waltham, MA, USA) using KBr pellet technique from 400 to 4000 cm^{-1}. X-ray photoelectron spectra were recorded on a PHI 5600 Multi-Technique XPS (Physical Electronics, Lake Drive East, Chanhassen, MN, USA) using monochromatized Al Ka at 1486.6 eV. Peak fitting was performed using CASA XPS Version 2.3.14 software, USA. CHNS analysis was carried out to estimate the nitrogen content in all the samples by using CHNS/O analyzer (2400 Series, Perkin Elmer, USA). The surface morphology of all the samples were analyzed by using Field emission scanning electron microscopy (FE-SEM) (Jeol, JED-2200 series (Akishima, Tokyo 196–8558, Japan)) with an acceleration voltage of 5–30 kV. The surface area of the NDG and NDG-Pd was measured using NOVA 4200e surface area and pore size analyzer (Quantachrome Instruments, FL, USA). The shape and dispersion of Pd NPs on the surface of NDG was analyzed using transmission electron microscope (Jeol TEM model JEM-1011 (Japan)) working at an accelerating voltage of 200 kV.

2.4. Electrocatalytic activity

Electrochemical measurements were performed using a three-electrode system using a Gamry Potentiostat (1010E). Ag/AgCl (3 M KCl) and Pt wire electrode were used as reference and counter electrodes respectively. All potentials were converted to reverse hydrogen electrode (RHE) values using the equation

$V_{RHE} = V_{Ag/AgCl} + 0.059*pH + 0.197$.

The electrodes were prepared using drop casting on a fluorinated tin oxide (FTO) glass support. The casting ink for each material was prepared by mixing 10 mg of the electrocatalyst by suspending in a 2 ml of an equimolar mixture of ethanol and deionized (DI). The suspension was mixed using ultrasonication for 2 h. 5 μL of Nafion solution (0.5 %) was added as binder. After the homogenous ink was prepared, 10 μL of the prepared ink was drop casted on a 1 × 1 cm^2 area of FTO substrate. The prepared electrodes were dried in an oven, first at 60 °C for one hour followed by 150 °C for another hour. The electrochemical measurements were performed in Pyrex glass electrochemical cell using 0.5 M H_2SO_4 electrolyte.

3. Results and discussion

Herein, ultrafine Pd NPs were successfully deposited on the surface of N-doped graphene (NDG-Pd) using a facile ultrasonic method to obtain hybrid electrocatalysts. In order to study the effect of Pd on the electrocatalytic properties of resulting nanocomposites, the Pd contents was varied to prepare three different hybrids consisting of 1 and 3 % of Pd on the surface of N-doped graphene. For this purpose, the N-doped graphene (NDG) was prepared by using GRO as precursor, which was reduced and doped simultaneously in a single-step hydrothermal

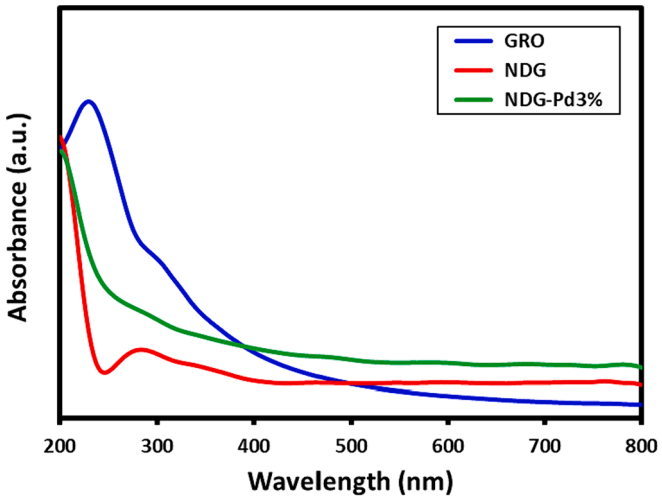

Fig. 1. UV–vis spectra of graphene oxide (GRO), nitrogen doped graphene (NDG) and palladium deposited NDG (NDG-Pd3%).

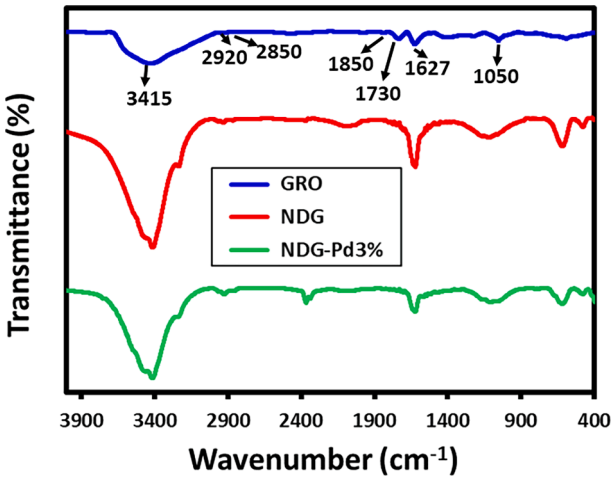

Fig. 2. FT-IR spectra of graphene oxide (GRO), nitrogen doped graphene (NDG) and palladium deposited NDG (NDG-Pd3%).

approach using NH_4OH as doping agent. In the beginning, the preparation of NDG-Pd was assessed via UV–Vis analysis as shown in Fig. 1, which exhibits the UV spectra of GRO (blue line), NDG (red line) and NDG-Pd with 3 % Pd (green line). The GRO exhibits two characteristic absorption at ~ 230 and ~ 300 nm, due to n–π* transitions of C = O bonds present in GRO, which are vanished in NDG, this confirms the reduction of GRO to NDG (Khan et al., 2015). On the other hand, the NDG shows a new absorption peak at ~ 275 nm, which points towards the reduction of GRO and the limited restoration of π network of NDG. While, in the case of NDG-Pd, only the absorption peak at ~ 275 nm, which represent NDG is present but, with reduced intensity, as Pd NPs do not exhibit any peak in the UV spectrum, therefore, their presence is confirm by other characterization technique.

Fig. 2 demonstrates the FT-IR spectra of GRO, NDG, and NDG-Pd. Several IR peaks are present in the FT-IR spectrum of GRO (blue line) which correspond to the different functional groups on its surface, including, carboxylic, hydroxyl, ether and ester and epoxy groups etc. These functional groups are represented by various IR peaks which are present at ~ 3415, ~2920, ~2850, ~1850, ~1730, ~1627, and ~ 1050 cm^{-1}, etc. For example, the broad peak at 3415 represents hydroxyl groups belonging to the vibration of phenolic and carboxylic moieties (C-OH), while the peaks between 2920 and 2850 correspond to methylene stretch of CH or CH_2 groups of GRO (Ren et al., 2010). On the other hand, the FT-IR peaks associated with the stretching vibrations of the ketonic species (C = O) of carbonyl and carboxylic groups appeared between 1600 and 1650 cm^{-1} and 1730 to 1850 cm^{-1}. These peaks in the GRO sample point towards the presence of many oxygen-containing functional groups. Whereas, in NDG, some of these peaks have either slightly shifted and merged with other peaks or their intensities were reduced due to the elimination of some of the functional groups after reduction, these changes indicate the successful reduction of GRO to NDG. On the other hand, in the case of NDG-Pd, apart from the similar IR peaks of NDG, two additional peaks are found at ~ 1325 and ~ 1570 cm^{-1} which typically corresponds to the C-N bond stretching arising from the secondary aromatic amine and represent the bonding between carbon and nitrogen atoms (Kuniyil et al., 2019).

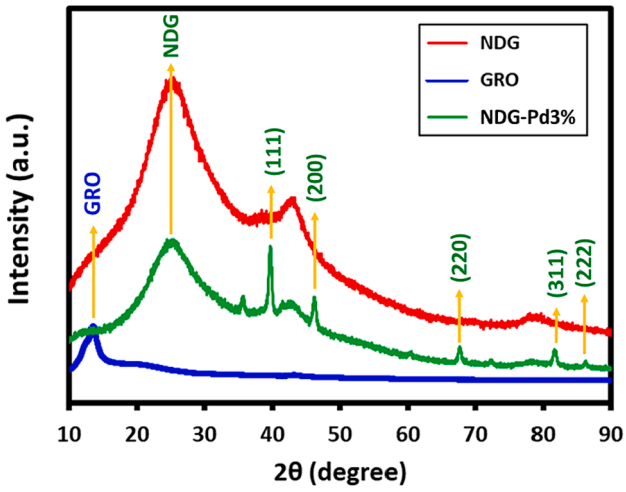

Fig. 3. XRD diffractograms of graphene oxide (GRO), nitrogen doped graphene (NDG) and palladium deposited NDG (NDG-Pd3%).

In addition, the crystallinity and formation of samples has been confirm using the XRD analysis, as shown in Fig. 3, which depicts the diffractograms of GRO (blue line), NDG (red line) and NDG-Pd3% (green line). Pristine graphite which is used as a precursor for the preparation of GRO, consists of a distinct and sharp diffraction peak at ~ 26.7°, which disappears upon oxidation due to the increase spacing between graphene layers by the incorporation of oxygenated groups. While, the successful oxidation of graphite is represented by the disappearance of the characteristic peak of graphite and the appearance of new peak at lower Bragg angle (Assal et al., 2017). Similarly, in this case, a characteristic GRO diffraction peak appeared at 2θ = 10.9° (Fig. 3, blue line), which clearly indicated towards the formation of GRO. While in the case of NDG (Fig. 3, red line) and NDG-Pd3% (Fig. 3, green line), the distinct GRO peak at 2θ = 10.9° disappeared while a new peak emerged at 2θ = 22.4°, which is an indication of the reduction of oxygenated groups and partial restoration of carbon skeleton in the samples. Notably, the absence of characteristic GRO peaks in the XRD diffractograms of NDG and NDG-Pd indicates the presence of reduced form of GRO, which was prepared in a single-step, in which simultaneous doping and reduction was achieved. Apart from the diffraction peaks of reduced form of GRO, the XRD diffractogram of NDG-Pd3% also consisted of several other peaks at different locations which possibly represent Pd NPs. Indeed, the position of these peaks i.e., at 2θ = 40.02° (111), 46.49° (200), 68.05° (220), 81.74° (311), and 86.24° (222) distinctly confirms the presence of *face-centered cubic* (*fcc*) structure of Pd NPs (JCPDS: 87–0641; space group: Fm3m (225)) (Kuniyil et al., 2019). These results point towards the formation of NDG-Pd.

The Brunauer–Emmett–Teller (BET) specific surface areas of the NDG and NDG-Pd were measured using the nitrogen adsorption–desorption isotherms at 77 K. The results revealed that, NDG demonstrated the specific surface area of ~ 366 m^2/g, while the

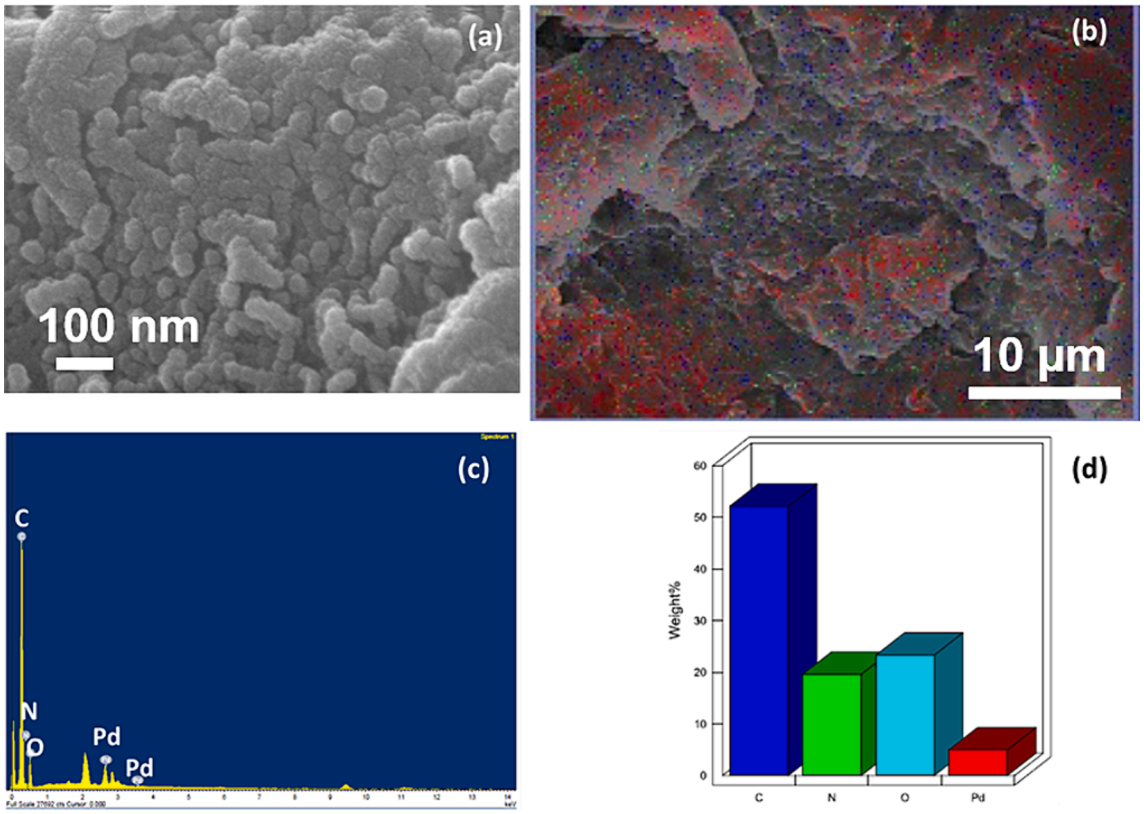

Fig. 4. (a) SEM image and (b) elemental mapping of NDG-Pd3% sample, which depicts the presence of different elements in the sample, including, carbon (red color), nitrogen (black color), oxygen (green color), and palladium (blue color), (c and d) EDX spectra and percentage of elements of the NDG-Pd3%.

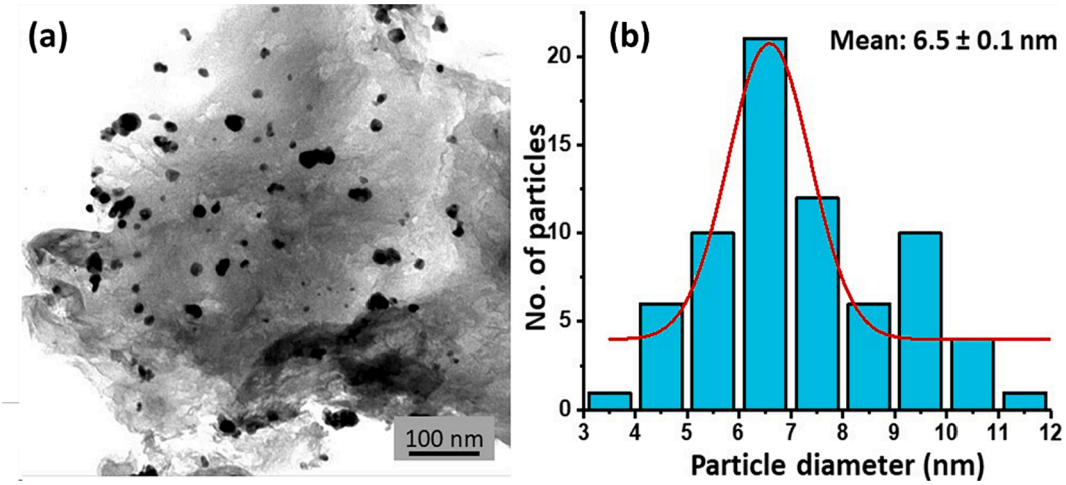

Fig. 5. (a) TEM image of NDG-Pd3% and (b) particle size distribution of the palladium nanoparticles on the surface of NDG.

palladium deposited NDG (NDG-Pd3%) showed relatively less surface area of ~ 278 m^2/g. The slight decrease in the surface area of NDG-Pd3% can be possibly attributed to the presence of Pd NPs, which may have been aggregated on the surface and reduced the interlayer spacing between the individual graphene layers. Still, the surface areas of both the samples obtained in this study are either much higher or almost similar when compare to the previously reported studies (Balaji and Sathish, 2014; Sheng et al., 2011). To further confirm the N doping and the amount of nitrogen contents present in the samples, the samples were subjected to CHN analysis. The NDG showed 5.46 % of nitrogen. The presence of nitrogen in both the samples were further confirmed by EDX and XPS analysis, whereas the morphology of the NDG and the Pd NPs on the surface of NDG was examined using SEM and TEM.

The scanning electron micrograph (Fig. 4a) showed pallidum nanoparticles dispersed NDG sheets. The nanocomposites appeared completely sheathed. The individual Pd nanoparticles or NDG sheets are not visible because of very small size and is beyond the resolution limits of microscope. However, SEM was very much helpful to find the chemical states of elements in NDG-Pd3% using EDX (Fig. 4b-d). Fig. 4b shows the elemental maps confirming the presence C, N and Pd. The Fig. 4c shows the EDX spectra of the samples. The presence of nitrogen is clearly indicated in the sample, while in addition to nitrogen, carbon and oxygen, palladium was detected. The relative atomic weight percentage was confirmed as presented in graphical image (Fig. 4d). The

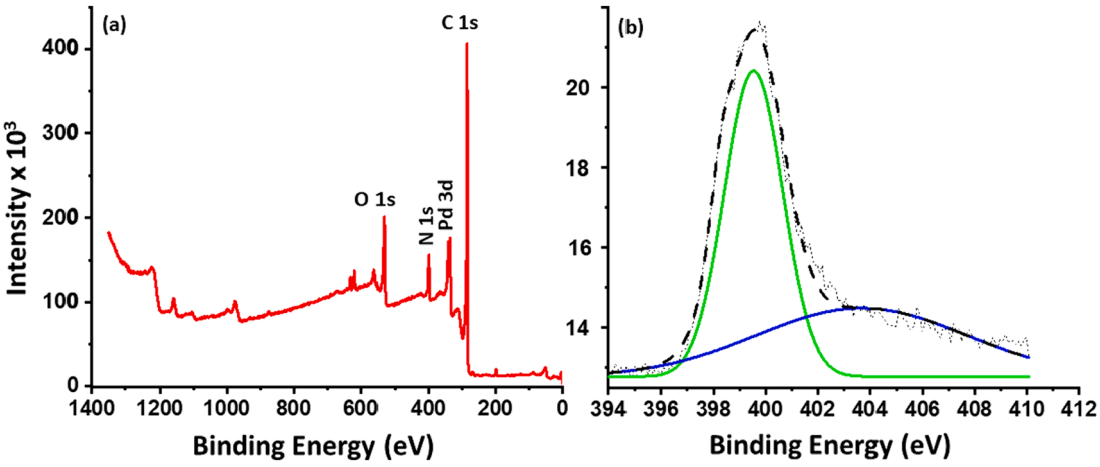

Fig. 6. (a) XPS survey spectrum of NDG-Pd3%, (b) N1s of the doped N.

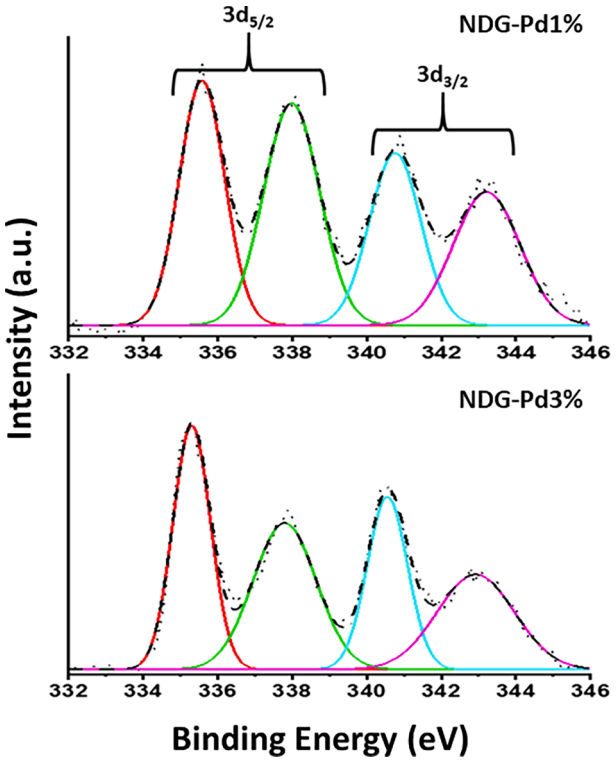

Fig. 7. Deconvoluted XPS spectra of three different composites including NDG-Pd1% and NDG-Pd3%. Note: the image exhibit only the Pd 3d region of the XPS spectra of these composite.

morphology was further confirmed by transmission electron microscopy (TEM) as shown in Fig. 5a. The TEM image clearly depicts the presence of crumbled, sheet like morphology. On the surface of crumbled graphene sheets, spherical shaped Pd NPs are dispersed with slight agglomeration, NPs are in the size range of 5 to 30 nm with an average diameter of ~ 6.5 nm.

XPS is an established technique to evaluate the characteristics of elements present in the samples, the XPS survey spectra of NDG-Pd (Fig. 6a) exhibit three eminent peaks at ~ 284.6, ~401 and ~ 532.3 eV which correspond to C1s of C, N1s of the doped N, and O1s, of the composite respectively (Balaji and Sathish, 2014). Deconvolution of N1s peak at ~ 401 eV (cf. Fig. 6b) clearly exhibits two peaks at 399.4 and 404.2 eV with a relative intensity of ~ 80 and 20 %, respectively. Typically, there are three kinds of N-doping namely pyridinic-N, pyrrolic-N and graphitic-N in graphene nanosheets which can identified based on their binding energies. In this case, out of these three different types of N-doping, the peak intensity observed for pyridinic-N is relatively much higher (~399.4 eV) which indicate that the N-doping in graphene skeleton is predominantly in the form of pyridinium nitrogen (~80 %). In order to demonstrate the state of palladium in three different composites, XPS spectra of the composites including NDG-Pd1%, and NDG-Pd3% were measured, and the deconvoluted spectra are shown in Fig. 7. According to the spectral data obtained from the high-resolution spectrum with regards to the Pd 3d region, there is a clear evidence of the presence of Pd(0) and Pd(II) moieties in all three nanocomposites (Zheng et al., 2022). The spectra generated signals corresponding to the ~ 335 eV and ~ 340 eV, which can be attributed to the presence of Pd(0) $3d_{5/2}$ and $3d_{3/2}$, respectively. Moreover, additional signals at ~ 338 eV and ~ 342 eV correspond to the existence of Pd(2 +) $3d_{5/2}$ and $3d_{3/2}$, respectively. The percentage composition of Pd(0) and Pd (2 +) can be understood from the intensity of the signals obtained and in the case of the 1 % the composition percentage of Pd(0) is 54 %, while in 3 % it is found to be 63 %. Thus, the percentage of Pd NPs is higher in the 3 % sample which may exhibit superior electrochemical properties. Apart from this, the XPS survey spectrum of NDG-Pd3% (cf. Fig. 6) demonstrates three distinguished peaks at 284.6, 401 and 532.3 eV corresponding to C1s of C, N1s of the doped N, and O1s, respectively. This points towards the successful doping of the graphene sheets with nitrogen (Balaji and Sathish, 2014).

The as prepared electrodes using NDG, NDG-Pd1% and NDG-Pd3% were measured for their potential to electrochemical hydrogen evolution reaction (HER) performance to produce hydrogen. Their electrocatalytic activity for the HER was monitored using linear sweep voltammetry (LSV) and cyclic voltammetry analysis. The electrochemical measurements were performed using a three-electrode system with Pt wire and Ag/AgCl (3 M KCl) electrode were used as counter and reference electrodes respectively. The measurements were performed using 0.5 M H_2SO_4 as electrolyte. The data obtained using electrochemical linear sweep voltammetry and cyclic voltammetry (CV) measurements is shown in Fig. 8. The CV results are presented in Fig. 8A. The CV plots showed within the voltage range measured nitrogen doped graphene did not show any current whereas NDG-Pd3% showed the best electrochemical current density. Similarly, the LSV plots (Fig. 8B) clearly showed that 3 % Pd-doped NDG has good potential for HER with current density ≈24 mA/cm^2 at very low potential i.e. −0.2 V vs RHE. It is worth mentioning that even dilution of Pd to 3 % supported on nitrogen doped graphene could produce current density of 10 mA even blow potential of −0.2 V vs RHE. The onset potential of 3 % Pd-NDG is much lower as compare to 1 % Pd or pristine NDG as shown in zoomed in LSV plots provided as supplementary materials (Fig. S1).

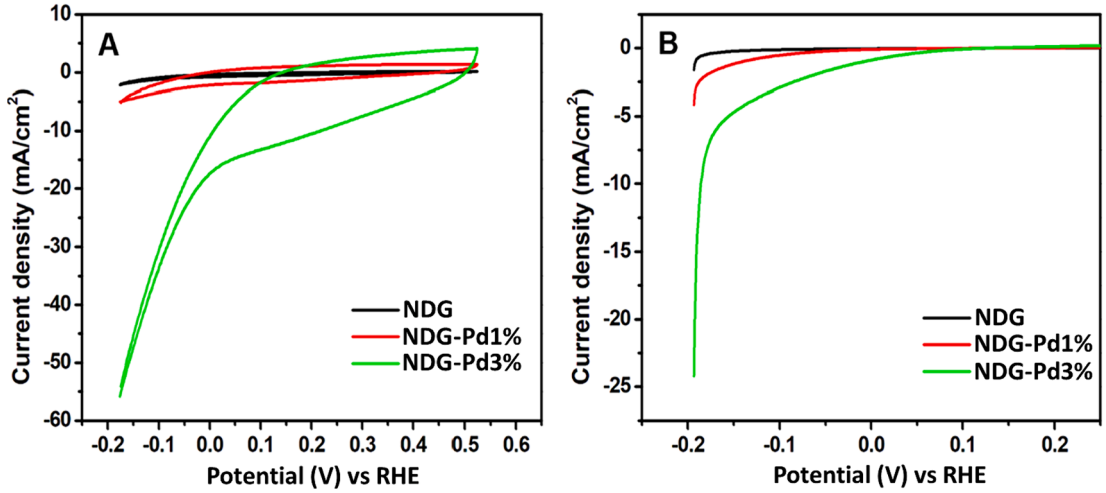

Fig. 8. Electrochemical measurements; (A) CV curves for NDG-Pd1% and NDG-Pd3%, and (B) LSV plots for NDG-Pd1% and NDG-Pd3%, in a 0.5 M H_2SO_4 electrolyte.

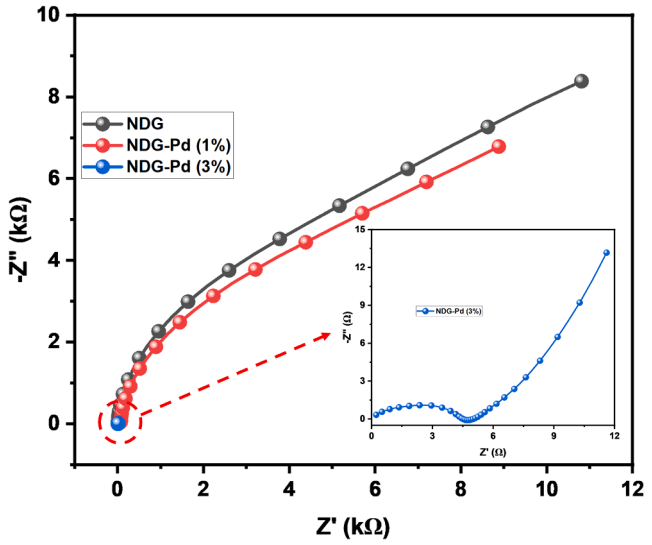

Fig. 9. Nyquist plots of NDG (black), NDG-Pd (1%), and NDG-Pd (3%).

The Electrochemical Impedance Spectroscopy (EIS) was measured in 0.5 M H_2SO_4 using three different electrodes: Nitrogen-Doped Graphene Oxide (NDG), Nitrogen-Doped Graphene Oxide with 1 % Pd (NDG/Pd (1 %)), and Nitrogen-Doped Graphene Oxide with 3 % Pd (NDG/Pd (3 %)). The EIS results revealed distinctive Nyquist plots for each electrode Fig. 9. Notably, the NDG/Pd (3 %) electrode exhibited the lowest semicircle (inset Fig. 9), indicative of a lower charge transfer resistance (R_{ct}) compared to NDG/Pd (1 %) and NDG. This observation suggests that the NDG/Pd (3 %) electrode possesses superior electrocatalytic activity for the HER. The trend of decreasing R_{ct} from NDG to NDG/Pd (1 %) to NDG/Pd (3 %) aligns with expectations. The incorporation of Pd nanoparticles enhances the electrocatalytic activity by providing active sites for the HER. The higher Pd loading in NDG/Pd (3 %) further improves the catalytic performance, resulting in the lowest R_{ct} among the tested electrodes. The lower Rct observed for NDG/Pd (3 %) implies faster charge transfer kinetics at the electrode–electrolyte interface, contributing to enhance HER performance. This finding is consistent with our LSV results.

4. Conclusions

The synthesis of novel electrocatalysts with tunable compositions, morphologies and electronic structures is fundamentally crucial for the fabrication of high-performance HER electrocatalysts. In this study, we have demonstrated the preparation of a new N-doped graphene and Pd nanoparticles based composite electrocatalyst using a facile ultrasonic method. During the preparation, nitrogen functionalities were obtained on the surface of graphene via doping leading to the homogeneous dispersion of smaller sized Pd NPs on the surface of graphene due to the great affinity between N and Pd. The nitrogen on the surface of graphene acted as active nucleation sites which facilitated the growth of Pd NPs. Besides, the N-doped graphene (NDG) in this case has also enhanced stability and electrocatalytic activity of the resulting composite catalyst. Indeed, the utilization of even smaller contents of palladium i.e., 1 and 3 wt% of the amount of NDG have exerted decent electrocatalytic property to the composites electrocatalysts towards electrochemical H_2 production. Among different samples, nitrogen doped graphene did not show any current whereas, NDG-Pd3% demonstrated superior electrochemical current density. Therefore, the composite of NDG with very small contents of Pd offers a viable alternative to the precious metals like Pt for the electrochemical H_2 production through water splitting.

Funding

The authors extend their appreciation to the Deputyship for Research & Innovation, “Ministry of Education” in Saudi Arabia for funding this research work through the project number (IFKSUDR_E120).

Declaration of competing interest

The authors declare that they have no known competing financial interests or personal relationships that could have appeared to influence the work reported in this paper.

Acknowledgments

The authors extend their appreciation to the Deputyship for Research & Innovation, “Ministry of Education” in Saudi Arabia for funding this research work through the project number (IFKSUDR_E120).

Appendix A. Supplementary data

Supplementary data to this article can be found online at https://doi.org/10.1016/j.arabjc.2024.105718.

References

Abbas, M.A., Bang, J.H., 2015. Rising again: opportunities and challenges for platinum-free electrocatalysts. Chem. Mater. 27, 7218–7235.

Adil, S.F., Ashraf, M., Khan, M., Assal, M.E., Shaik, M.R., Kuniyil, M., Al-Warthan, A., Siddiqui, M.R.H., Tremel, W., Tahir, M.N., 2022. Advances in graphene/inorganic nanoparticle composites for catalytic applications. The Chemical Record 22, e202100274.

Al-Rawashdeh, N.A., Albiss, B.A., Mo'Ath, H., 2018. In *graphene-based transparent electrodes for dye sensitized solar cells*. IOP Conference Series: Materials Science and Engineering, IOP Publishing, 012019.

Ashraf, M., Shah, S.S., Khan, I., Aziz, M.A., Ullah, N., Khan, M., Adil, S.F., Liaqat, Z., Usman, M., Tremel, W., 2021. A high-performance asymmetric supercapacitor based on tungsten oxide nanoplates and highly reduced graphene oxide electrodes. Chem. Eur. J. 27, 6973–6984.

Ashraf, M., Ali, R., Khan, I., Ullah, N., Ahmad, M.S., Kida, T., Wooh, S., Tremel, W., Schwingenschlögl, U., Tahir, M.N., 2023a. Bandgap engineering of melon using highly reduced graphene oxide for enhanced photoelectrochemical hydrogen evolution. Adv, Mater, p. 2301342.

Ashraf, M., Ayaz, M., Khan, M., Adil, S.F., Farooq, W., Ullah, N., Nawaz Tahir, M., 2023b. Recent trends in sustainable solar energy conversion technologies: mechanisms, prospects, and challenges. Energy & Fuels 37, 6283–6301.

Ashraf, M., Ullah, N., Khan, I., Tremel, W., Ahmad, S., Tahir, M.N., 2023c. Photoreforming of waste polymers for sustainable hydrogen fuel and chemicals feedstock: waste to energy. Chem. Rev. 123, 4443–4509.

Assal, M.E., Shaik, M.R., Kuniyil, M., Khan, M., Al-Warthan, A., Siddiqui, M.R.H., Khan, S.M., Tremel, W., Tahir, M.N., Adil, S.F., 2017. A highly reduced graphene oxide/ZrO_x–$MnCO_3$ or–Mn_2O_3 nanocomposite as an efficient catalyst for selective aerial oxidation of benzylic alcohols. RSC Adv. 7, 55336–55349.

Balaji, S.S., Sathish, M., 2014. Supercritical fluid processing of nitric acid treated nitrogen doped graphene with enhanced electrochemical supercapacitance. RSC Adv. 4, 52256–52262.

Chen, X., Wu, G., Chen, J., Chen, X., Xie, Z., Wang, X., 2011. Synthesis of "clean" and well-dispersive pd nanoparticles with excellent electrocatalytic property on graphene oxide. J. Am. Chem. Soc. 133, 3693–3695.

Chen, S., Xu, J., Chen, J., Yao, Y., Wang, F., 2024. Current Progress of mo-based metal organic frameworks derived electrocatalysts for hydrogen evolution reaction. Small 20, 2304681.

Dharmarajan, N.P., Vidyasagar, D., Yang, J.H., Talapaneni, S.N., Lee, J., Ramadass, K., Singh, G., Fawaz, M., Kumar, P., Vinu, A., 2024. Bio-inspired supramolecular self-assembled carbon nitride nanostructures for photocatalytic water splitting. Adv. Mater. 36, 2306895.

Duan, J., Chen, S., Jaroniec, M., Qiao, S.Z., 2015. Heteroatom-doped graphene-based materials for energy-relevant electrocatalytic processes. ACS Catal. 5, 5207–5234.

Dumont, J.H., Martinez, U., Artyushkova, K., Purdy, G.M., Dattelbaum, A.M., Zelenay, P., Mohite, A., Atanassov, P., Gupta, G., 2019. Nitrogen-doped graphene oxide electrocatalysts for the oxygen reduction reaction. ACS Appl. Nano Mater. 2, 1675–1682.

Fajrina, N., Tahir, M., 2019. A critical review in strategies to improve photocatalytic water splitting towards hydrogen production. Int. J. Hydrogen Energy 44, 540–577.

Gao, G., Chen, X., Han, L., Zhu, G., Jia, J., Cabot, A., Sun, Z., 2024. Advances in MOFs and their derivatives for non-noble metal electrocatalysts in water splitting. Coord. Chem. Rev. 503, 215639.

Gupta, J., Das, D., Borse, P.H., Bulusu, S.V., 2024. In-situ pd doped MoS_2 nanosheets as HER electrocatalyst for enhanced electrocatalytic water splitting. sustainable. Energy & Fuels.

Han, D., Hao, L., Wang, R., Gao, Y., Su, M., Zhang, Y., 2024. Design yolk-shelled FeCo layered double hydroxide via a "one-stone-two-birds" strategy for oxygen evolution reaction. Sep. Purif. Technol. 336, 126363.

Hanan, A., Lakhan, M.N., Bibi, F., Khan, A., Soomro, I.A., Hussain, A., Aftab, U., 2024. MOFs coupled transition metals, graphene, and MXenes: emerging electrocatalysts for hydrogen evolution reaction. Chem, Eng. J, p. 148776.

Hassan, Q., Viktor, P., Al-Musawi, T.J., Ali, B.M., Algburi, S., Alzoubi, H.M., Al-Jiboory, A.K., Sameen, A.Z., Salman, H.M., Jaszczur, M., 2024. The renewable energy role in the global energy transformations. Renewable Energy Focus 48, 100545.

Hayden, B.E., 2013. Particle size and support effects in electrocatalysis. Acc. Chem. Res. 46, 1858–1866.

Huang, K., Hao, L., Liu, Y., Su, M., Gao, Y., Zhang, Y., 2024. Facile synthesis of FeNi alloy-supported N-doped Mo_2C hollow nanospheres for the oxygen evolution reaction. J. Colloid Interface Sci. 658, 267–275.

Hussain, A., Arif, S.M., Aslam, M., 2017. Emerging renewable and sustainable energy technologies: state of the art. Renew. Sust. Energ. Rev. 71, 12–28.

Ibn Shamsah, S.M., 2021. Earth-abundant electrocatalysts for water splitting: current and future directions. Catalysts 11, 429.

Jeong, S., Mai, H.D., Nam, K.-H., Park, C.-M., Jeon, K.-J., 2022. Self-healing graphene-templated platinum–nickel oxide heterostructures for overall water splitting. ACS Nano 16, 930–938.

Jiang, Y., Fu, H., Liang, Z., Zhang, Q., Du, Y., 2024. Rare earth oxide based electrocatalysts: synthesis, properties and applications. Chem. Soc, Rev.

Jiao, Y., Zheng, Y., Davey, K., Qiao, S.-Z., 2016. Activity origin and catalyst design principles for electrocatalytic hydrogen evolution on heteroatom-doped graphene. Nature Energy 1, 1–9.

Khan, M., Al-Marri, A.H., Khan, M., Shaik, M.R., Mohri, N., Adil, S.F., Kuniyil, M., Alkhathlan, H.Z., Al-Warthan, A., Tremel, W., 2015. Green approach for the effective reduction of graphene oxide using Salvadora persica L. root (miswak) extract. Nanoscale Research Letters 10, 1–9.

Khan, I., Baig, N., Bake, A., Haroon, M., Ashraf, M., Al-Saadi, A., Tahir, M.N., Wooh, S., 2023. Robust electrocatalysts decorated three-dimensional laser-induced graphene for selective alkaline OER and HER. Carbon 213, 118292.

Khan, M., Shaik, M.R., Adil, S.F., Kuniyil, M., Ashraf, M., Frerichs, H., Sarif, M.A., Siddiqui, M.R.H., Al–Warthan, A., Labis, J.P., 2020. Facile synthesis of PD@ graphene nanocomposites with enhanced catalytic activity towards Suzuki coupling reaction. Sci. Rep. 10, 11728.

Kim, H., Yoo, T.Y., Bootharaju, M.S., Kim, J.H., Chung, D.Y., Hyeon, T., 2022. Noble metal-based multimetallic nanoparticles for electrocatalytic applications. Adv. Sci. 9, 2104054.

Kuniyil, M., Kumar, J.S., Adil, S.F., Shaik, M.R., Khan, M., Assal, M.E., Siddiqui, M.R.H., Al-Warthan, A., 2019. One-pot synthesized PD@ N-doped graphene: an efficient catalyst for Suzuki-miyaura couplings. Catalysts 9, 469.

Li, Y., Tsang, S.C.E., 2020. Recent progress and strategies for enhancing photocatalytic water splitting. Materials Today Sustainability 9, 100032.

Li, Y., Wei, X., Chen, L., Shi, J., 2021. Electrocatalytic hydrogen production trilogy. Angew. Chem. Int. Ed. 60, 19550–19571.

Lin, L., Hisatomi, T., Chen, S., Takata, T., Domen, K., 2020. Visible-light-driven photocatalytic water splitting: recent progress and challenges. Trends in Chemistry 2, 813–824.

Liu, X., Chen, W., Zhang, X., 2022. Highly active palladium-decorated reduced graphene oxides for heterogeneous catalysis and electrocatalysis: hydrogen production from formaldehyde and electrochemical formaldehyde detection. Nanomaterials 12, 1890.

Liu, P., Li, G., Chang, W.-T., Wu, M.-Y., Li, Y.-X., Wang, J., 2015. Highly dispersed pd nanoparticles supported on nitrogen-doped graphene with enhanced hydrogenation activity. RSC Adv. 5, 72785–72792.

Liu, M., Lu, Y., Chen, W., 2013. PdAg nanorings supported on graphene nanosheets: highly methanol-tolerant cathode electrocatalyst for alkaline fuel cells. Adv. Funct. Mater. 23, 1289–1296.

Lyu, F., Wang, Q., Choi, S.M., Yin, Y., 2019. Noble-metal-free electrocatalysts for oxygen evolution. Small 15, 1804201.

Ma, J., Li, X., Lei, G., Wang, J., Wang, J., Liu, J., Ke, M., Li, Y., Sun, C., 2024. A general synthetic strategy for N, P co-doped graphene supported metal-rich noble metal phosphides for hydrogen generation. Green Energy & Environment 9, 152–162.

Mahesh, K.N., Balaji, R., Dhathathreyan, K., 2016. Palladium nanoparticles as hydrogen evolution reaction (HER) electrocatalyst in electrochemical methanol reformer. Int. J. Hydrogen Energy 41, 46–51.

Margarit, C.G., Asimow, N.G., Thorarinsdottir, A.E., Costentin, C., Nocera, D.G., 2021. Impactful role of cocatalysts on molecular electrocatalytic hydrogen production. ACS Catal. 11, 4561–4567.

Narreddula, M., Balaji, R., Ramya, K., Rajalakshmi, N., Ramachandraiah, A., 2019. Nitrogen doped graphene supported pd as hydrogen evolution catalyst for electrochemical methanol reformation. Int. J. Hydrogen Energy 44, 4582–4591.

Qazi, A., Hussain, F., Rahim, N.A., Hardaker, G., Alghazzawi, D., Shaban, K., Haruna, K., 2019. Towards sustainable energy: a systematic review of renewable energy sources, technologies, and public opinions. IEEE Access 7, 63837–63851.

Rauf, S., Irfan, M., Hayat, A., Alghamdi, M.M., El-Zahhar, A., Ghernaout, D., Al-Hadeethi, Y., Lv, W., 2024. Recent developments, advances, strategies in heterogeneous photocatalysts for water splitting. Nanoscale Adv 6, 1286–1330.

Ren, P.-G., Yan, D.-X., Ji, X., Chen, T., Li, Z.-M., 2010. Temperature dependence of graphene oxide reduced by hydrazine hydrate. Nanotechnology 22, 055705.

Saini, R., Naaz, F., Bashal, A.H., Pandit, A.H., Farooq, U., 2024. Recent advances in nitrogen-doped graphene-based heterostructures and composites: mechanism and active sites for electrochemical ORR and HER. Green Chem 26, 57–102.

Shen, T., Zhang, J., Chen, K., Deng, S., Wang, D., 2020. Recent progress of palladium-based electrocatalysts for the formic acid oxidation reaction. Energy & Fuels 34, 9137–9153.

Sheng, Z.-H., Shao, L., Chen, J.-J., Bao, W.-J., Wang, F.-B., Xia, X.-H., 2011. Catalyst-free synthesis of nitrogen-doped graphene via thermal annealing graphite oxide with melamine and its excellent electrocatalysis. ACS Nano 5, 4350–4358.

Sikiru, S., Oladosu, T.L., Amosa, T.I., Olutoki, J.O., Ansari, M., Abioye, K.J., Rehman, Z. U., Soleimani, H., 2024. Hydrogen-powered horizons: transformative technologies in clean energy generation, distribution, and storage for sustainable innovation. Int. J. Hydrogen Energy 56, 1152–1182.

Smiljanić, M., Grgur, B., 2024. Advanced electrocatalytic materials for water electrolysis and fuel cells. Frontiers Media SA 12, 1373189.

Sun, H., Xu, X., Kim, H., Shao, Z., Jung, W., 2024. Advanced electrocatalysts with unusual active sites for electrochemical water splitting. InfoMat 6, e12494.

Tang, Y., Cheng, W., 2015. Key parameters governing metallic nanoparticle electrocatalysis. Nanoscale 7, 16151–16164.

Vogt, C., Weckhuysen, B.M., 2022. The concept of active site in heterogeneous catalysis. Nature Reviews Chemistry 6, 89–111.

Wang, T., Chutia, A., Brett, D.J., Shearing, P.R., He, G., Chai, G., Parkin, I.P., 2021. Palladium alloys used as electrocatalysts for the oxygen reduction reaction. Energy & Environmental Science 14, 2639–2669.

Wang, S., Liu, G., Wang, L., 2019. Crystal facet engineering of photoelectrodes for photoelectrochemical water splitting. Chem. Rev. 119, 5192–5247.

Yi, S.-S., Zhang, X.-B., Wulan, B.-R., Yan, J.-M., Jiang, Q., 2018. Non-noble metals applied to solar water splitting. Energy & Environmental Science 11, 3128–3156.

Yue, M., Lambert, H., Pahon, E., Roche, R., Jemei, S., Hissel, D., 2021. Hydrogen energy systems: a critical review of technologies, applications, trends and challenges. Renew. Sust. Energ. Rev. 146, 111180.

Zhang, W., Dai, L., 2024. Mesoporous metal nanomaterials: developments and electrocatalytic applications. Chem, Eur. J, p. e202400402.
Zhang, J., Zhang, Q., Feng, X., 2019. Support and interface effects in water-splitting electrocatalysts. Adv. Mater. 31, 1808167.
Zhang, J., Hao, L., Chen, Z., Gao, Y., Wang, H., Zhang, Y., 2023. Facile synthesis of Co–Fe layered double hydroxide nanosheets wrapped on ni-doped nanoporous carbon nanorods for oxygen evolution reaction. J. Colloid Interface Sci. 650, 816–824.
Zhang, L., Jia, C., Bai, F., Wang, W., An, S., Zhao, K., Li, Z., Li, J., Sun, H., 2024. A comprehensive review of the promising clean energy carrier: hydrogen production, transportation, storage, and utilization (HPTSU) technologies. Fuel 355, 129455.
Zhao, Y., Ling, T., Chen, S., Jin, B., Vasileff, A., Jiao, Y., Song, L., Luo, J., Qiao, S.Z., 2019. Non-metal single-iodine-atom electrocatalysts for the hydrogen evolution reaction. Angew. Chem. Int. Ed. 58, 12252–12257.
Zheng, F., Kwong, T.-L., Yung, K.-F., 2022. Surfactant-free monodispersed pd nanoparticles template for core-shell PD@ pdpt nanoparticles as electrocatalyst towards methanol oxidation reaction (mor). Nanomaterials 12, 260.
Zhong, Y., Lu, Y., Pan, Z., Yang, J., Du, G., Chen, J., Zhang, Q., Zhou, H., Wang, J., Wang, C., 2021. Efficient water splitting system enabled by multifunctional platinum-free electrocatalysts. Adv. Funct. Mater. 31, 2009853.